Growth of mutual information in a quenched one-dimensional open quantum many-body system

Somnath Maity, Souvik Bandyopadhyay, Sourav Bhattacharjee and Amit Dutta

Department of Physics, Indian Institute of Technology Kanpur, Kanpur 208016, India

We study the temporal evolution of the mutual information (MI) in a one-dimensional Kitaev chain, coupled to a fermionic Markovian bath, subsequent to a global quench of the chemical potential. In the unitary case, the MI (or equivalently the bipartite entanglement entropy) saturates to a steady-state value (obeying a volume law) following a ballistic growth. On the contrary, we establish that in the dissipative case the MI is exponentially damped both during the initial ballistic growth as well as in the approach to the steady state. We observe that even in a dissipative system, post quench information propagates solely through entangled pairs of quasi-particles having a finite life time; this quasi-particle picture is further corroborated by the out-of-equilibrium analysis of two-point fermionic correlations. Remarkably, in spite of the finite life time of the quasi-particles, a finite steady-state value of the MI survives in asymptotic times which is an artefact of non-vanishing two points correlations. Further, the finite life time of quasi-particles renders to a finite length scale in these steady-state correlations.

The mutual information (MI) is an important measure of the amount of correlations present in a quantum system. For a pure composite state, it is equivalent with the bipartite entanglement entropy (EE), which is the more commonly used tool for probing purely quantum correlations. The EE has a wide range of applications in areas ranging from quantum computation [1] and quantum many body physics [2–4] to conformal field theory [5], quantum gravity [6] and black holes [7]. In condensed matter physics, for example, the EE can be used to probe quantum criticality [8] and complexity [9]. The scaling behaviour of the EE enables us to distinguish quantum phases that cannot be characterized by symmetry properties, such as topological phases of matter [10–12] and spin liquids [13, 14]. Experimental studies [15] probing the purity of the reduced system under consideration, firmly establish the entropic measures of many-body entanglement, both in and out of equilibrium, on physical grounds. The underlying aspect that makes the EE relevant in such diverse areas as listed above is intricately tied to the following fundamental question: how do quantum correlations propagate in a system under different incumbent situations?

If the composite system is pure, the bipartite EE is calculated through the von Neumman entropy of the reduced density matrix ρ_ℓ for a sub-system of size ℓ;

$$S(\ell) = -\mathrm{Tr}\left[\rho_\ell \ln \rho_\ell\right], \qquad (1)$$

where $\rho_\ell = \mathrm{Tr}_{L-\ell}\left[\rho_L\right]$ and ρ_L is the density matrix of the composite system of size L. For a short-range one-dimensional Hamiltonian with a gapped spectrum, the EE follows an area law [8, 16], while a logarithmic scaling exists for the gapless phase [8].

Recently, there has been great interest in studying the temporal evolution of the EE of an isolated quantum many body system following a quantum quench in which a parameter of the Hamiltonian is changed [17–43]. The out-of-equilibrium dynamics of the system results in the propagation of quantum correlations over the whole system thus leading to a growth of non-trivial bipartite entanglement even if the initial state is completely unentangled. It has been established [18] that following a global quench of a one-dimensional free fermionic Hamiltonian, $S(\ell, t)$ exhibits a ballistic growth, $S(\ell, t) \sim t$, up to a time $t^* = \ell/2v_{\max}$, where $v_{\max}$ is the maximum group velocity of information propagation determined by the so-called Lieb-Robinson bound [44]. (see also [45]). This 'light-cone' like spreading of correlations has also been experimentally demonstrated in Ref. [46]. For $t > t^*$, $S(\ell, t)$ saturates to a constant value proportional to ℓ, and hence the EE satisfies a volume law in the steady-state.

However, all the studies of the EE carried out so far fundamentally assumes an isolated or non-dissipative setting. This is simply because the EE itself is known to quantify bipartite entanglement when the composite system is pure. On the contrary, the presence of at least minimal dissipation in any physical system is inevitable. The purpose of our work is thus to investigate this unexplored area, namely how do correlations propagate in an out-of-equilibrium quantum many body system in the presence of a weak *dissipative* environment. The first necessary step to address in this regard is to define an appropriate measure similar to the EE to probe the propagation of correlations. Since the composite system is in a mixed state in the dissipative situation, the bipartite EE as defined in Eq. (1) is naturally no longer significant as a measure of entanglement unlike the unitary case. We therefore define another measure which, as we show, is equivalent to the mutual information (MI) [1]. Although the MI is not guaranteed to strictly encode only quantum correlations [47], it nevertheless reproduces the results of the quantum correlations manifested in the EE at least in the non-dissipative limit, thereby permitting a critical comparison between the two scenarios. Furthermore, the dynamics of MI has also recently been studied in the con-

text of quantum information scrambling after a quantum quench [48]. The second question we address is whether the dissipative coupling to the bath results in an instantaneous (space like) propagation of correlations, thus violating the Lieb-Robinson bound. Although, for a general Markov process with short-ranged interactions, a Lieb-Robinson-like limit has been shown to exist [49], and is indeed corroborated by our results, a concrete physical picture, particularly in terms of propagating quasi-particles is not yet established. Finally, we also explore the fate of the correlations in the asymptotic steady-state of the system. In this regard, we note that some works [50, 51] have revealed the existence of short-range as well as long-range correlations in the asymptotic steady states of a dissipative system; however, the dynamical emergence of these asymptotic steady-state correlations remains unexplored. Our work addresses these less understood areas which are crucial to gain a better understanding of how the dissipative behavior emerge from the well understood unitary settings.

Mutual informartion– The MI is defined as [1]:

$$I(\ell : L - \ell) = S(\rho_\ell) + S(\rho_{L-\ell}) - S(\rho_L), \qquad (2)$$

where $S(\rho_\ell)$, $S(\rho_{L-\ell})$, and $S(\rho_L)$ are the von Neumann entropies of the sub-system, the rest of the system and the composite system, respectively. For a pure composite system, $S(\rho_L) = 0$ and $S(\rho_\ell) = S(\rho_{L-\ell})$; consequently, the MI remains equivalent to the bipartite EE for the unitary evolution, provided the initial state is pure. However, for a mixed ρ_L, $S(\rho_\ell) \neq S(\rho_{L-\ell}) \neq I(\ell : L - \ell)/2$.

By splitting the quantity $S(\rho_L)$ into two parts, we can rewrite Eq. (2) as

$$I(\ell : L - \ell) = S'(\ell) + S'(L - \ell), \qquad (3)$$

where

$$S'(\ell) = S(\rho_\ell) - \frac{\ell}{L} S(\rho_L), \qquad (4)$$

$$S'(L - \ell) = S(\rho_{L-\ell}) - \frac{L - \ell}{L} S(\rho_L). \qquad (5)$$

Interestingly, in our case, $S'(\ell) = S'(L - \ell) = I(\ell : L - \ell)/2$ (see [52] for verification). In hindsight, this factorization of $S(\rho_L)$ is meaningful when the Lindbladian operators act independently on each site with uniform coupling strengths.

Model and the bath– In this work, we consider a one-dimensional Kitaev chain *globally* coupled to a Markovian bath (see Ref. [52] for details) and model the dynamical evolution of this system within a Lindbladian framework [53–55]. The Kitaev Hamiltonian [56] (see also Ref. [57] and references therein) we work with is,

$$H = -\sum_{n=1}^{L} \left(c_n^\dagger c_{n+1} - c_n c_{n+1} + h.c. \right) - \mu \sum_{n=1}^{L} \left(2c_n^\dagger c_n - 1 \right); \qquad (6)$$

where c_n ($c_n^\dagger$) are the fermionic annihilation (creation) operators acting on the nth site. The chain is prepared in the unentangled ground state of the Hamiltonian with a large negative value of the on-site potential (μ) which is instantaneously quenched to the final critical value $\mu_f = 1$. We note that this model can also be mapped to the transverse field Ising model through a Jordan-Wigner transformation [58–63]. Following a Fourier transformation to the quasi-momentum (k) basis, the Hamiltonian decouples to the form: $H = \sum_{k>0} H_k$, where H_k assumes a 4×4 form (see Ref. [52]).

We choose a specific Markovian bath where the system-bath interaction is characterized by a set of Lindblad operators $\mathcal{L}_n = c_n, \forall n$ [64–67]. The efficacy of such a choice of Lindbladian operator is that in the case of homogenous coupling strengths ($\kappa_n = \kappa, \forall n$), the Lindblad master equation (with $\hbar = 1$) gets decoupled in the momentum modes as

$$\frac{d\rho_k(t)}{dt} = -i[H_k, \rho_k(t)] + \mathcal{D}_k[\rho_k(t)], \qquad (7)$$

with

$$\mathcal{D}_k[\rho_k(t)] = \kappa \Big(c_k \rho_k(t) c_k^\dagger - \frac{1}{2} \left\{ c_k^\dagger c_k, \rho_k(t) \right\} + c_{-k} \rho_k(t) c_{-k}^\dagger - \frac{1}{2} \left\{ c_{-k}^\dagger c_{-k}, \rho_k(t) \right\} \Big) (8)$$

where $\rho_k(t)$ is the 4×4 time evolved density matrix, $c_k^\dagger$ is the fermionic creation operator for the mode k and $\rho(t) = \otimes_{k>0} \rho_k(t), \forall t$.

Numerical results– The system is initially prepared in the unentangled ground state of the Hamiltonian $H_k(\mu)$ with $\mu \to -\infty$. At $t = 0+$, the on-site potential μ is suddenly changed to the critical value $\mu_f = 1$ and the system evolves with the final Hamiltonian $H(\mu_f)$ following Eq. (7). Numerically evaluating $\rho_k(t)$, we arrive at the two point correlations (TPCs) of fermions;

$$C_{mn}(t) = \text{Tr}\left[\rho(t), c_m^\dagger c_n\right], \quad F_{mn}(t) = \text{Tr}\left[\rho(t), c_m^\dagger c_n^\dagger\right] (9)$$

where $m, n = 1, 2, \ldots, \ell$. Finally, diagonalizing the $2\ell \times 2\ell$ correlation matrix

$$\mathbb{C}_\ell = \begin{pmatrix} I - C & F \\ F^\dagger & C \end{pmatrix} \qquad (10)$$

for the sub-system of size ℓ, one can calculate $S(\rho_\ell, t)$ and hence the MI ($S'(\ell, t)$) for a free fermionic model [68] (see Ref. [52]).

Unitary situation: For $\kappa = 0$ [18], the temporal evolution of the MI is reproduced in Fig. 1(a). Indeed, the MI shows a ballistic growth up to a time $t^* = \ell/2$ and subsequently saturates to a constant value which is proportional to ℓ. We note that in the limit $L \to \infty$, $\ell \to \infty$ with $\ell \ll L$, the MI is expected to have a ballistic growth indefinitely in time. On the contrary, for any finite ℓ, the MI follows the $\ell \to \infty$ line only up to
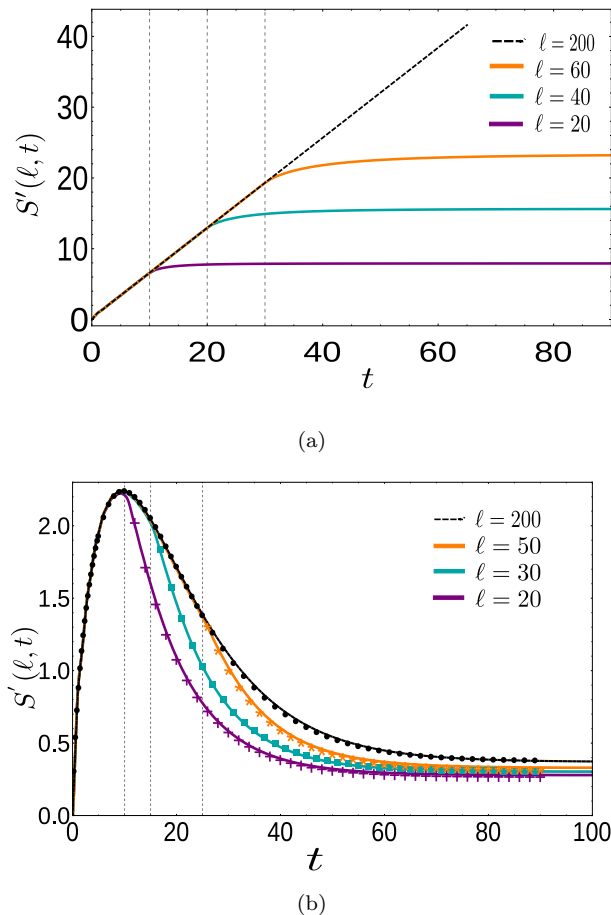
(a)

(b)

FIG. 1. (Color online) The time evolution of $S'(\ell,t)$ for (a) $\kappa = 0$ and (b) $\kappa = 0.05$ with different sub-system size ℓ. The black dashed line is for a large $\ell = 200$ and indicates the results in the limit $\ell \to \infty$ (with $\ell \ll L$). In (b), the markers denote the plots using the fitting functions defined in Eq. (11) for $t < \ell/2$ and Eq. (12) for $t > \ell/2$ as discussed in the text. Here, in both cases (a) and (b), the total system size $L = 500$.

the time $t = t^* = \ell/2$. This behaviour of the MI has been explained by a semiclassical description in terms of entangled pair of quasi-particles with equal and opposite group velocities v with $v_{\max} = 1$, resulting in a light-cone like spread of correlations [44]. Further, the steady-state saturation of the MI is an artifact of the infinite life time of the quasi particles, although similar behavior has also been observed in a non-integrable model, where presumably information does not propagate through ballistically moving quasi-particles [70].

Dissipative situation: We now proceed to the case $\kappa \neq 0$; the temporal variation of $S'(\ell,t)$, obtained from Eq. (4) using $\rho_k(t)$, is presented in Fig. 1(b) for different sub system sizes ℓ. Critically inspecting the results, we conclude that the temporal evolution of $S'(\ell,t)$ is significantly different when compared to that of the MI with $\kappa = 0$. For a given ℓ, we observe a monotonic non-linear growth of the entanglement after which it eventually de-

cays to the steady-state value. The difference with the $\kappa = 0$ situation is even more prominent in the limit $L \to \infty$, $\ell \to \infty$ with $\ell \ll L$, where, unlike the indefinite ballistic growth of MI expected in the former case, $S'(\ell,t)$ is found to decay to a finite (ℓ-independent) steady value following the initial growth. However, similar to the case $\kappa = 0$, the deviation of $S'(\ell,t)$ from $S'(\ell \to \infty, t)$ again occurs at the same instant $t = \ell/2$.

We propose the the following functional form of $S'(\ell,t)$ in the limit $\ell \to \infty$,

$$S'(\ell \to \infty, t) \sim \mathcal{A}\left(1 - e^{-c(\kappa)t}\right) + \mathcal{B}te^{-d(\kappa)t}, \quad (11)$$

with $c(\kappa) \gg d(\kappa)$ and the parameter $\mathcal{B}$ is a non-universal constant depending on the group velocity of quasi-particles. Eq. (11) gives a perfect fitting with the numerically obtained results (see Fig. 1(b)). The functional form can be interpreted in the following way: In early times, $S'(\ell \to \infty, t) \sim \mathcal{B}te^{-d(\kappa)t}$, which essentially means that the linear growth in the MI observed in the $\kappa = 0$ situation is now exponentially suppressed. This suppression can be attributed to the finite life-time of the quasi-particles in the case of finite dissipation. However, a finite MI survives in the asymptotic steady state, $S'(\ell \to \infty, t \to \infty) = \mathcal{A}$. As argued below that, surprisingly, this remanent MI is due to perpetual coupling with the bath.

Following the insight obtained from the $\kappa = 0$ situation, it is natural to expect that for a finite ℓ, the early time growth of the MI ($\sim te^{-d(\kappa)t}$) will continue as long as the quasi-particles originating from the center of the sub-system do not cross the sub-system boundary, following which the MI will only decay exponentially, i.e., $\sim e^{-d(\kappa)t}$. This is what we indeed observe in Fig. 1(b). We therefore arrive at a modified functional form for $t > \ell/2$,

$$S'(\ell,t) \sim \mathcal{P}(\ell,\kappa) + \frac{\mathcal{B}\ell}{2}e^{-d(\kappa)t} \quad , \quad (12)$$

which again fits perfectly with the numerical results [Fig. 1(b)]. The steady state value $\mathcal{P}(\ell,\kappa)$ approaches $\mathcal{A}$ in the limit $\ell \to \infty$; this steady value satisfies an area law resulting from a finite correlation length ξ_k defined below.

Two-point correlations– At this point, a proper analysis of the influence of the bath on the TPCs given in Eq. (9) is instrumental in understanding the behavior of the $S'(\ell,t)$ presented above. We note that the same for a quantum XXZ chain has already been studied [69].

For a translationally invariant system with periodic boundary conditions, the single particle TPC, $C_{mn}(t)$, between sites m and n, depends on the distance between the two sites (either $|m-n|$ or $L - |m-n|$). In Fig. 2, we plot the temporal evolution of $C_{mn}(t)$ for different values of κ. For the unitary case ($\kappa = 0$), a finite correlation begins to develop only after a time
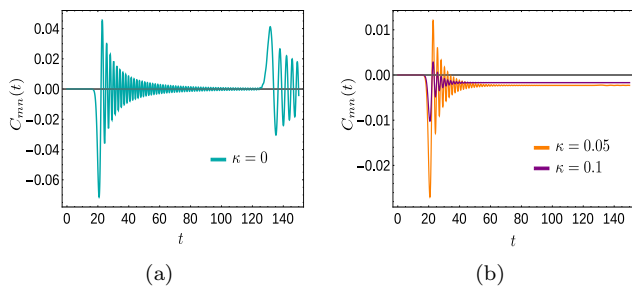
FIG. 2. (Color online) This figure shows the time evolution of the two point correlation $C_{mn}(t)$ for (a) $\kappa = 0$ and (b) $\kappa = 0.05, 0.1$ under the quenching protocol ($\mu = -\infty$ to $\mu = 1$). We have considered two fixed sites m and n with $|m-n| = 40$, and $L = 300$.

FIG. 3. (Color online) Here, we have plotted the quantity $\ln(|C_{mn}(\infty)|)$ scaled by κ with respect to $(m - n)$. This shows a linear behaviour for all κ having a slope equal to 0.5, suggesting an exponential decay [Eq. (13)] of the steady state TPCs.

$t = \min\{|(m - n)/2|, |(L - m + n)/2|\}$. The existence of a finite correlation between the two sites 'm' and 'n' at a particular instant of time can now be attributed to the arrival of one quasi-particle of an entangled pair at site m and the other at site n at the same time. This evidently ensures that *only* the quasi-particles originating at the middle of either of the two segments between the two points can contribute to TPCs. Since the minimum time taken by these quasi-particles to arrive at the two sites is given by $t^* = \min\{|(m - n)/2|, |(L - m + n)/2|\}$, no finite correlation is observed for $t < t^*$. The successive peaks occur due to the slower moving quasi-particles ($v(k) < v_{\max}$). The slower moving quasi-particles are less abundant than the faster moving ones, as evident from the progressively decreasing amplitude of the subsequent peaks. A revival of correlation can occur due to the arrival of the quasi-particles from the middle of the longer segment connecting the two points [see Fig. 2(a)]. We note that in the thermodynamic limit $L \to \infty$ and for a finite $|m - n| \ll L$, this revival can not occur.

Importantly, even for the case $\kappa \neq 0$, no finite correlation is observed for $t < t^*$. As already mentioned, we note that the maximum velocity of the quasi particles is the same as in the unitary case. The amplitudes of the correlations are also smaller as compared to the $\kappa = 0$ case with the amplitude of the revivals significantly diminished. This supports the fact that the quasi particles originating at $t = 0$ now have a finite life time. Further, the two-point correlation saturates to a finite non zero value unlike the $\kappa = 0$ situation [Fig. 2(b)]. This is manifested also in the non zero steady-state value of the $S'(\ell, \infty)$ as analyzed in Ref. [52].

Finally, the steady-state TPC when plotted as a function of the (shorter) intermediate distance $|m - n|$, (see Fig. 3) shows an exponential decay of the form,

$$C_{mn}(\infty) \sim \exp\left\{-\frac{\kappa(m - n)}{2}\right\}. \qquad (13)$$

This implies that when $|n - m|$ exceeds $2/\kappa$, the quasi-particles generate negligible correlations, thereby point-
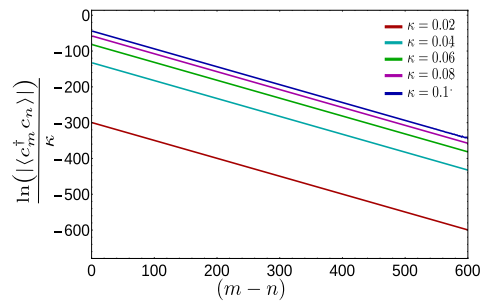
ing to a finite length scale, $\xi_\kappa = 2/\kappa$, of the steady state TPCs.

The above analysis of the TPCs has the following bearing on the behaviour of $S'(\ell, t)$ discussed earlier. Since the group velocity of the entangled pair of quasi particles remains unaltered for $\kappa \neq 0$, we observe that the deviation in $S'(\ell, t)$ from the $\ell \to \infty$ curve occurs at $t^* = \ell/2$ as for $\kappa = 0$. The remanent TPC in the steady state is reflected in the non zero steady-state value of $S'(\ell, t)$. This steady-state MI , however, results from the collective contribution of remanent TPCs between sites that are located within a finite distance ($\sim \xi_\kappa$) from either end of the sub system. The remanent TPCs can be attributed to a *continuous* generation of quasi-particles due to perpetual coupling with the bath as discussed in Ref. [52]. We note that this is significantly different from the $\kappa = 0$ case where the finite MI at large time is maintained collectively by TPCs between all sites of the system. Further, the finite life time of quasi-particles results in an exponential suppression of the MI at all instants of time.

In summary, we study the influence of a weak dissipative coupling on the generation and growth of the MI in a quenched one-dimensional integrable model. As in the unitary ($\kappa = 0$) case, the MI acquires a finite steady value at long times; in this case, however, the steady value is determined by both the post quench Hamiltonian as well as the coupling strength with the bath and follows an area law in the thermodynamic limit. Moreover, the ballistic growth due to the quench-induced propagating correlations is exponentially damped due to the bath-induced dissipation.

To conclude, a scope for further research would be to consider a more general dissipative environment, including thermal as well as non-Markovian baths (see also Ref. [71]). Further, studying the interplay between non-integrability and dissipation to probe the fate of the ballistic growth in Ref. [70] is a challenging problem.

————

[1] M. A. Nielsen and I. L. Chuang, *Quantum Computation and Information*, (Cambridge University Press, Cambridge, U.K., 2010).

[2] L. Amico, R. Fazio, A. Osterloh, and V. Vedral, Entanglement in many-body systems, Rev.Mod.Phys., **80**, 517 (2008).

[3] J. I. Latorre, A. Riera, A short review on entanglement in quantum spin systems, J. Phys. A: Math. Theor. **42** (2009) 504002.

[4] J. Eisert, M. Cramer, and M. B. Plenio, Colloquium: Area laws for the entanglement entropy, Rev. Mod. Phys. **82**, 277 (2010).

[5] P. Calabrese, and J. Cardy, Entanglement entropy and conformal field theory, J. Phys. A: Math. Theor. **42**, 504005 (2009).

[6] T. Nishioka, S. Ryu, and T. Takayanagi, Holographic entanglement entropy: An overview, J. Phys. A: Math. Theor. **42**, 504008 (2009).

[7] S. N. Solodukhin, Entanglement entropy of black holes, Living Rev. Relativity **14**, 8 (2011).

[8] G. Vidal, J. I. Latorre, E. Rico, and A. Kitaev, Entanglement in Quantum Critical Phenomena, Phys. Rev. Lett. **90**, 227902 (2003).

[9] N. Schuch, M. M. Wolf, F. Verstraete, and J. I. Cirac, Entropy Scaling and Simulability by Matrix Product States, Phys. Rev. Lett. **100**, 030504 (2008).

[10] A. Kitaev and J. Preskill, Topological Entanglement Entropy, Phys. Rev. Lett. **96**, 110404 (2006).

[11] M. Levin and X.-G. Wen, Detecting Topological Order in a Ground State Wave Function, Phys. Rev. Lett. **96**, 110405 (2006).

[12] H.-C. Jiang, Z. Wang and L. Balents, Identifying topological order by entanglement entropy, Nature Phys. **8**, 902?905 (2012).

[13] Y. Zhang, T. Grover and A. Vishwanath, Entanglement Entropy of Critical Spin Liquids, Phys. Rev. Lett.107, 067202 (2011).

[14] S. V. Isakov, M. B. Hastings and R. G. Melko, Topological entanglement entropy of a BoseHubbard spin liquid, Nature Phys. **7**, 772775 (2011).

[15] R. Islam, R. Ma, P. M. Preiss, M. E. Tai, A. Lukin, M. Rispoli, Measuring entanglement entropy in a quantum many-body system, M. Greiner, Nature **528**, 77 (2015).

[16] P. Calabrese and J. Cardy, Entanglement entropy and quantum field theory, J. Stat. Mech.: Theory Exp. **2004**, P06002.

[17] A. Polkovnikov, K. Sengupta, A. Silva, and M. Vengalattore, Colloquium: Nonequilibrium dynamics of closed interacting quantum systems, Rev. Mod. Phys. **83**, 863 (2011).

[18] P. Calabrese, and J. Cardy, Evolution of entanglement entropy in one-dimensional systems, J. Stat. Mech.: Theory Exp. **2005**, P04010.

[19] M. Fagotti, and P. Calabrese, Evolution of entanglement entropy following a quantum quench: Analytic results for the XY chain in a transverse magnetic field , Phys. Rev. A **78**, 010306 (R) (2008).

[20] I. Pitsios, L. Banchi, A. S. Rab, M. Bentivegna, D. Caprara, A. Crespi, N. Spagnolo, S. Bose, P. Mataloni, R. Osellame, F. Sciarrino., Photonic simulation of entanglement growth and engineering after a spin chain quench, Nat. Commun. **8**, 1569 (2017).

[21] G. D. Chiara, S Montangero, P. Calabrese, and R Fazio, Entanglement Entropy dynamics in Heisenberg chains, J. Stat. Mech.: Theory Exp. **2006**, P03001.

[22] C. K. Burrell and T. J. Osborne, Bounds on the Speed of Information Propagation in Disordered Quantum Spin Chains, Phys. Rev. Lett. **99**, 167201 (2007).

[23] V. Eisler and I. Peschel, Evolution of entanglement after a local quench, J. Stat. Mech.: Theory Exp. **2007**, P06005.

[24] P. Calabrese and J. Cardy, Entanglement and correlation functions following a local quench: a conformal field theory approach, J. Stat. Mech.: Theory Exp. **2007**, P10004.

[25] V. Eisler, D Karevski, T Platini, and I Peschel, Entanglement evolution after connecting finite to infinite quantum chains, J. Stat. Mech.: Theory Exp. **2008**, P01023.

[26] V. Eisler and I. Peschel, Entanglement in a periodic quench, Ann. Phys. (Berlin) **17**, 410 (2008).

[27] M. Znidaric, T. Prosen, and P. Prelovsek, Many-body localization in the Heisenberg XXZ magnet in a random field, Phys. Rev. B **77**, 064426 (2008).

[28] Jean-Marie Stephan, and Jerome Dubail, Local quantum quenches in critical one-dimensional systems: entanglement, the Loschmidt echo, and light-cone effects, J. Stat. Mech.: Theory Exp. **2011**, P08019.

[29] U. Divakaran, F. Igloi and H. Ruger, Non-equilibrium quantum dynamics after local quenches, J. Stat. Mech.: Theory Exp. **2011**, 10027.

[30] F. Igli, Z. Szatmri, and Y. Lin, Entanglement entropy dynamics of disordered quantum spin chains, Phys. Rev. B **85**, 094417 (2012).

[31] J. H. Bardarson, F. Pollmann, and J. E. Moore, Unbounded Growth of Entanglement in Models of Many-Body Localization, Phys. Rev. Lett. **109**, 017202 (2012).

[32] R. Vosk and E. Altman, Dynamical Quantum Phase Transitions in Random Spin Chains, Phys. Rev. Lett. **112**, 217204 (2014).

[33] P. Ponte, Z. Papi, F. Huveneers, and D. A. Abanin, Many-Body Localization in Periodically Driven Systems, Phys. Rev. Lett. **114**, 140401 (2015).

[34] A. Rajak, and U. Divakaran, Effect of double local quenches on the Loschmidt echo and entanglement entropy of a one-dimensional quantum system, J. Stat. Mech.: Throry Exp. **2016**, 043107.

[35] A. Sen, S. Nandy, and K. Sengupta, Entanglement generation in periodically driven integrable systems: Dynamical phase transitions and steady state, Phys. Rev. B **94**, 214301 (2016).

[36] A. Russomanno, G. E. Santoro and R. Fazio, Entanglement entropy in a periodically driven Ising chain, J. Stat. Mech.: Theory Exp. **2016**, 073101.

[37] T. J. G. Apollaro, G. M. Palma, and J. Marino, Entanglement entropy in a periodically driven quantum Ising ring , Phys. Rev. B **94**, 134304 (2016).

[38] S. Nandy, A. Sen, and D. Sen, Aperiodically Driven Integrable Systems and Their Emergent Steady States, Phys. Rev. X 7, 031034 (2017).

[39] U. Bhattacharya, S. Maity, U. Banik, and A. Dutta, Ex-

act results for the Floquet coin toss for driven integrable models, Phys. Rev. B **97**, 184308 (2018).

[40] S. Maity, U. Bhattacharya, and A. Dutta, Fate of current, residual energy, and entanglement entropy in aperiodic driving of one-dimensional Jordan-Wigner integrable models Phys. Rev. B **98**, 064305 (2018).

[41] S. Nandy, A. Sen, and D. Sen, Steady states of a quasiperiodically driven integrable system , Phys. Rev. B **98** 245144 (2018).

[42] L. Cincio, J. Dziarmaga, M. M. Rams, and W. H. Zurek, Entropy of entanglement and correlations induced by a quench: Dynamics of a quantum phase transition in the quantum Ising model, Phys. Rev. A 75, 052321 (2007).

[43] E. Canovi, E. Ercolessi, P. Naldesi, L. Taddia, and D. Vodola, Dynamics of entanglement entropy and entanglement spectrum crossing a quantum phase transition, Phys. Rev. B 89, 104303 (2014).

[44] E.H. Lieb and D.W. Robinson, The finite group velocity of quantum spin systems, Commun. Math. Phys. **28**, 251 (1972).

[45] The ballistic growth of entanglement can also be precisely characterized by the *entanglement tsunami velocity*, whose maxima correspond to the Lieb-Robinson bound. see, H. Casini, H. Liu, and M. Mezei, Spread of entanglement and causality. J. High Energ. Phys. 2016, 77 (2016). https://doi.org/10.1007/JHEP07(2016)077

[46] M. Cheneau, *et al.*, Light-cone-like spreading of correlations in a quantum many-body system, Nature (London) **481**, 484 (2012).

[47] B. Groisman, S. Popescu, and A. Winter, Quantum, classical, and total amount of correlations in a quantum state, Phys Rev A, **72**, 032317 (2005).

[48] V. Alba and P. Calabrese, "Quantum information scrambling after a quantum quench", Phys. Rev. B **100**, 1151502 (2019).

[49] D. Poulin, Lieb-Robinson Bound and Locality for General Markovian Quantum Dynamics, Phys. Rev. Lett. **104**, 190401 (2010)

[50] T. Prosen and I. Pizorn, Quantum Phase Transition in a Far-from-Equilibrium Steady State of an XY Spin Chain, Phys. Rev. Lett. **101**, 105701 (2008).

[51] T. Prosen and B. Zunkovic, Exact solution of Markovian master equations for quadratic Fermi systems: thermal baths, open XY spin chains and non-equilibrium phase transition, New Journal of Physics **12** 025016 (2010).

[52] See Supplemental Material for details of the model and bath, solution of $\rho_k(t)$, calculation of TPCs, and the steady-state behavior of the MI.

[53] G. Lindblad, On the generators of quantum dynamical semigroups, Commun. Math. Phys. **48**, 199 (1976).

[54] C. W. Gardiner and P. Zoller, *Quantum Noise* (Springer, Heidelberg, 2000).

[55] H. P. Breuer and F. Petruccione, *Theory of open quantum systems*, (Oxford University Press, Oxford, U.K., 2002).

[56] A. Kitaev, Unpaired Majorana fermions in quantum wires, Physics-Uspekhi **44**, 131 (2001).

[57] S. Maity, U. Bhattacharya and A. Dutta, One-dimensional quantum many body systems with long-range interactions, Journal of Physics A: Math. and Theo. **53** 013001(2019).

[58] E. Lieb, T. Schultz, and D. Mattis, Two soluble models of an antiferromagnetic chain, Ann. Phys. 16, 407 (1961).

[59] J. B. Kogut, An introduction to lattice gauge theory and spin systems, Rev. Mod. Phys. 51, 659 (1979).

[60] S. Sachdev, *Quantum Phase Transition*, (Cambridge University Press, Cambridge, U.K., 2011).

[61] S. Suzuki, J. Inoue, and B. K. Chakrabarti, *Quantum Ising Phases and Transitions in Transverse Ising Models*, Lecture Notes in Physics Vol. 862 (Springer, Berlin, 2013).

[62] A. Dutta, G. Aeppli, B. K. Chakrabarti, U. Divakaran,T. F. Rosenbaum, D. Sen, *Quantum Phase Transitions in Transverse Field Spin Models*, (Cambridge University Press, Cambridge, U.K., 2015).

[63] Results presented in this work will be identical to those of the transverse Ising chain following a similar sudden quench of the transverse field.

[64] A. Carmele, M. Heyl, C. Kraus, M. Dalmonte, Stretched exponential decay of Majorana edge modes in many-body localized Kitaev chains under dissipation, Phys. Rev. B **92**, 195107 (2015).

[65] M. Keck, S. Montangero, G. E. Santoro, R. Fazio, D. Rossini, Dissipation in adiabatic quantum computers: lessons from an exactly solvable model, New J. Phys. **19** 113029 (2017).

[66] S. Bandyopadhyay, S. Laha, U. Bhattacharya and A. Dutta, Exploring the possibilities of dynamical quantum phase transitions in the presence of a Markovian bath, Sci. Rep. **8**, 11921 (2018).

[67] S Bandyopadhyay, S Bhattacharjee, and A Dutta, Dynamical generation of Majorana edge correlations in a ramped Kitaev chain coupled to nonthermal dissipative channels, Phys. Rev. B **101**, 104307 (2020).

[68] I. Peschel, Calculation of reduced density matrices from correlation functions, J. Phys. A: Math. Gen. **36**, L205-L208 (2003).

[69] S. Wolff, J.-S. Bernier, D. Poletti, A. Sheikhan, and C. Kollath, Evolution of two-time correlations in dissipative quantum spin systems: Aging and hierarchical dynamics, Phys. Rev. B **100**, 165144 (2019).

[70] H. Kim, David A. Huse, Ballistic Spreading of Entanglement in a Diffusive Nonintegrable System, Phys. Rev. Lett. **111**, 127205 (2013).

[71] A similar study has also been recently reported by V. Alba and F. Carollo, Spreading of correlations in Markovian open quantum systems, arXiv:2002.09527 (2020).

Supplemental Material on "Growth of mutual information in a critically quenched one-dimensional open quantum many body system"

MODEL AND THE BATH

In this work, the subsequent dissipative dynamics of the Kitaev chain following a quench of the chemical potential (from $\mu = -\infty$ and $\mu = 1$) is assumed to be described by a Lindblad master equation of the form[S1–3],

$$\frac{d\rho(t)}{dt} = -i\left[H, \rho(t)\right] + \mathcal{D}\left[\rho(t)\right]; \tag{S1}$$

we have set $\hbar = 1$ througout. The first term on the right hand side describes the unitary time evolution evolution of the system's density matrix $\rho(t)$ while the dissipator $\mathcal{D}\left[\rho(t)\right]$ encapsulates the dissipative dynamics and assumes a form:

$$\mathcal{D}\left[\rho(t)\right] = \sum_n \kappa_n \left(\mathcal{L}_n \rho(t)\mathcal{L}_n^\dagger - \frac{1}{2}\left\{\mathcal{L}_n^\dagger \mathcal{L}_n, \rho(t)\right\}\right), \tag{S2}$$

where $\mathcal{L}_n$ are the Lindblad operators with κ_n (≥ 0)'s being the corresponding dissipation strengths.

The Kitaev chain is described by the Hamiltonian

$$H = -\sum_{n=1}^{L}\left(c_n^\dagger c_{n+1} - c_n c_{n+1} + h.c.\right) - \mu \sum_{n=1}^{L}\left(2c_n^\dagger c_n - 1\right); \tag{S3}$$

where c_n ($c_n^\dagger$) are Fermionic annihilation (creation) operators residing on the n-th site. Further, in the quasi-momentum basis, the Hamiltonian decouples as $H = \sum_{k>0} H_k$, with $k = \left[2\pi(n + 1/2)\right]/L$ where $n \in \{0, 1, 2 \ldots (L - 1)\}$. In the basis spanned by the states $\{|\phi_1^k\rangle = |0\rangle, |\phi_2^k\rangle = c_k^\dagger |0\rangle, |\phi_3^k\rangle = c_{-k}^\dagger |0\rangle, |\phi_4^k\rangle = c_k^\dagger c_{-k}^\dagger |0\rangle\}$, H_k assumes the form

$$H_k = \begin{pmatrix} \mu - \cos k & 0 & 0 & \sin k \\ 0 & 0 & 0 & 0 \\ 0 & 0 & 0 & 0 \\ \sin k & 0 & 0 & -\mu + \cos k \end{pmatrix}. \tag{S4}$$

For a specific system-bath interaction, as used in this work, characterised by a set of *local* Lindblad operators $\mathcal{L}_n = c_n$ [S4, 5], the Lindblad master equation given in Eq. (S1) decouples in the momentum modes as

$$\frac{d\rho_k(t)}{dt} = -i\left[H_k, \rho_k(t)\right] + \mathcal{D}_k\left[\rho_k(t)\right], \tag{S5}$$

with

$$\mathcal{D}_k\left[\rho_k(t)\right] = \kappa \left(c_k \rho_k(t)c_k^\dagger - \frac{1}{2}\left\{c_k^\dagger c_k, \rho_k(t)\right\} + c_{-k}\rho_k(t)c_{-k}^\dagger - \frac{1}{2}\left\{c_{-k}^\dagger c_{-k}, \rho_k(t)\right\}\right). \tag{S6}$$

In the next section, we will cast the Eq. (S5) into a set of coupled differential equations in a particular choice of basis and solve the them numerically to find out $\rho_k(t)$ in the present scenario .

GENERAL SOLUTION OF $\rho(t)$

In this section, we will briefly elaborate the calculation of the density matrix $\rho_k(t)$ for each momenta mode using the Eq. (S5)[S5, 6]. Let us recall the basis which we considered here,

$$|\phi_1^k\rangle \equiv |0, 0\rangle, \tag{S7}$$

$$|\phi_2^k\rangle \equiv c_k^\dagger |0, 0\rangle = |k, 0\rangle, \tag{S8}$$

$$|\phi_3^k\rangle \equiv c_{-k}^\dagger |0, 0\rangle = |0, -k\rangle, \tag{S9}$$

$$|\phi_4^k\rangle \equiv c_k^\dagger c_{-k}^\dagger |0, 0\rangle = |k, -k\rangle, \tag{S10}$$

where $|0,0\rangle$ and $|k,-k\rangle$ refer both the fermionic states for c_k and c_{-k} are occupied and unoccupied, respectively. In the above basis, we have the following matrix forms of c_k, c_{-k} and $H_k(h)$ for each k mode

$$c_k = \begin{pmatrix} 0 & 1 & 0 & 0 \\ 0 & 0 & 0 & 0 \\ 0 & 0 & 0 & -1 \\ 0 & 0 & 0 & 0 \end{pmatrix}, \qquad c_{-k} = \begin{pmatrix} 0 & 0 & 1 & 0 \\ 0 & 0 & 0 & 1 \\ 0 & 0 & 0 & 0 \\ 0 & 0 & 0 & 0 \end{pmatrix}, \quad \text{and} \quad H_k(h) = \begin{pmatrix} h - \cos k & 0 & 0 & \sin k \\ 0 & 0 & 0 & 0 \\ 0 & 0 & 0 & 0 \\ \sin k & 0 & 0 & -h + \cos k \end{pmatrix}. \tag{S11}$$

Using the above equations, the Lindblad equation (Eq. [10] in the main text) for each k mode contains sixteen coupled first order linear differential equations of which only ten are independent, those are

$$\dot{\rho}_{11}(t) = -i\Delta\left(\rho_{14}^\star(t) - \rho_{14}(t)\right) + \kappa\left(\rho_{22}(t) + \rho_{33}(t)\right),$$

$$\dot{\rho}_{12}(t) = -i\left(\epsilon\rho_{12}(t) + \Delta\rho_{24}^\star(t)\right) - \kappa\left(\frac{1}{2}\rho_{12}(t) - \rho_{34}(t)\right),$$

$$\dot{\rho}_{13}(t) = -i\left(\epsilon\rho_{13}(t) + \Delta\rho_{34}^\star(t)\right) - \kappa\left(\frac{1}{2}\rho_{13}(t) - \rho_{24}(t)\right),$$

$$\dot{\rho}_{14}(t) = -i\left(2\epsilon\rho_{14}(t) + \Delta\rho_{11}(t) + \Delta\rho_{44}(t)\right) - \kappa\rho_{14}(t),$$

$$\dot{\rho}_{22}(t) = -\kappa\rho_{22}(t) + \kappa\rho_{44}(t),$$

$$\dot{\rho}_{23}(t) = -\kappa\rho_{23}(t),$$

$$\dot{\rho}_{24}(t) = -i\left(\epsilon\rho_{24}(t) - \Delta\rho_{12}^\star(t)\right) - \frac{3\kappa}{2}\rho_{24}(t),$$

$$\dot{\rho}_{33}(t) = -\kappa\rho_{33}(t) + \kappa\rho_{44}(t),$$

$$\dot{\rho}_{34}(t) = -i\left(\epsilon\rho_{34}(t) - \Delta\rho_{13}^\star(t)\right) - \frac{3\kappa}{2}\rho_{34}(t),$$

$$\dot{\rho}_{44}(t) = -i\Delta\left(\rho_{14}(t) - \rho_{14}^\star(t)\right) - 2\kappa\rho_{44}(t). \tag{S12}$$

where $\epsilon = \mu - \cos k$, $\Delta = \sin k$ and $\dot{\rho}_{ij} = d\rho_{ij}/dt$. Solving the above equations we can obtain $\rho_k(t)$. It is evident from the above equations that if we consider the initial state prepared at $\mu_i = -\infty$ i.e., $\rho_k(0) = |0,0\rangle\langle 0,0|$, the density matrix $\rho_k(t)$ has only five non-zero elements, $\rho_{11}(t)$, $\rho_{22}(t)$, $\rho_{33}(t)$, $\rho_{44}(t)$, and $\rho_{14}(t)$. Thus, at any instant of time t, the density matrix for each k mode takes the following form

$$\rho_k(t) = \begin{pmatrix} \rho_{11}(t) & 0 & 0 & \rho_{14}(t) \\ 0 & \rho_{22}(t) & 0 & 0 \\ 0 & 0 & \rho_{33}(t) & 0 \\ \rho_{14}^\star(t) & 0 & 0 & \rho_{44}(t) \end{pmatrix}. \tag{S13}$$

Having the solutions of $\rho_k(t)$, we can proceed to calculate the fermionic two point correlations (TPCs) and eventually the mutual information (MI) $S'(\ell, t)$.

CALCULATION OF FERMIONIC TWO POINT CORRELATIONS

We now present the calculation of fermionic two point correlation functions using the density matrix $\rho_k(t)$. Let us first write the Fourier transform of fermion c_n for the momenta $k > 0$

$$c_n = \frac{1}{\sqrt{L}} \sum_{k>0} \left(e^{-ikn} c_k + e^{ikn} c_{-k}\right). \tag{S14}$$

Using the Eq. (S14), one can write the two point correlations (TPCs) in real space in terms of TPCs in the momentum space as

$$\langle c_m^\dagger c_n \rangle = \frac{1}{L} \sum_{k_1,k_2>0} \left(e^{i(k_1 m - k_2 n)}\langle c_{k_1}^\dagger c_{k_2}\rangle + e^{i(k_1 m + k_2 n)}\langle c_{k_1}^\dagger c_{-k_2}\rangle + e^{-i(k_1 m + k_2 n)}\langle c_{-k_1}^\dagger c_{k_2}\rangle + e^{-i(k_1 m - k_2 n)}\langle c_{-k_1}^\dagger c_{-k_2}\rangle\right),$$

$$\langle c_m^\dagger c_n^\dagger \rangle = \frac{1}{L} \sum_{k_1,k_2>0} \left(e^{i(k_1 m + k_2 n)}\langle c_{k_1}^\dagger c_{k_2}^\dagger\rangle + e^{i(k_1 m - k_2 n)}\langle c_{k_1}^\dagger c_{-k_2}^\dagger\rangle + e^{-i(k_1 m - k_2 n)}\langle c_{-k_1}^\dagger c_{k_2}^\dagger\rangle + e^{-i(k_1 m + k_2 n)}\langle c_{-k_1}^\dagger c_{-k_2}^\dagger\rangle\right), \tag{S15}$$

where all the expectation values on the right hand side are taken over the momentum space density matrix $\rho(t) = \otimes_{k>0}\rho_k(t)$ i.e. for a general operator $\hat{O}$;

$$\langle \hat{O}(t)\rangle = \text{Tr}\left[\rho(t)\hat{O}\right] = \sum_{k>0}\sum_{i,j=1}^{4} \rho_{i,j}^{k}(t)\,\langle \phi_j^k|\,\hat{O}\,|\phi_i^k\rangle. \tag{S16}$$

Using the Eq. (S16) and Eqs. (S7)-(S10), one can calculate the following correlations in momentum space;

$$\langle c_{k_1}^\dagger c_{k_2}\rangle = \sum_{k>0}\sum_{i,j=1}^{4} \rho_{i,j}^k\,\langle \phi_j^k|\,c_{k_1}^\dagger c_{k_2}\,|\phi_i^k\rangle = \sum_{k>0}\left(\rho_{22}^k + \rho_{44}^k\right)\delta_{k_1,k_2}\delta_{k_1,k}, \tag{S17}$$

$$\langle c_{-k_1}^\dagger c_{-k_2}\rangle = \sum_{k>0}\left(\rho_{33}^k + \rho_{44}^k\right)\delta_{k_1,k_2}\delta_{k_1,k}, \tag{S18}$$

$$\langle c_{k_1}^\dagger c_{-k_2}\rangle = \sum_{k>0}\left(\rho_{32}^k\right)\delta_{k_2,k}\delta_{k_1,k}, \tag{S19}$$

$$\langle c_{-k_1}^\dagger c_{k_2}\rangle = \sum_{k>0}\left(\rho_{23}^k\right)\delta_{k_2,k}\delta_{k_1,k}, \tag{S20}$$

and

$$\langle c_{k_1}^\dagger c_{k_2}^\dagger\rangle = 0, \tag{S21}$$

$$\langle c_{-k_1}^\dagger c_{-k_2}^\dagger\rangle = 0, \tag{S22}$$

$$\langle c_{k_1}^\dagger c_{-k_2}^\dagger\rangle = \sum_{k>0}\left(\rho_{14}^k\right)\delta_{k_2,k}\delta_{k_1,k}, \tag{S23}$$

$$\langle c_{-k_1}^\dagger c_{k_2}^\dagger\rangle = -\sum_{k>0}\left(\rho_{14}^k\right)\delta_{k_2,k}\delta_{k_1,k}. \tag{S24}$$

Note that in the last equation the negative sign comes from fermionic anti-commutation relations i.e. using the fact $c_{-k}^\dagger c_k^\dagger\,|0,0\rangle = -\,|k,-k\rangle$. Finally, using the above correlation functions in Eqs. (S17)-(S24) and Eq. (S15), the elements in the correlation matrix $\mathcal{C}$ for the sub system of size ℓ can be found as

$$C_{mn}(t) = \frac{1}{L}\sum_{k>0}\left(\rho_{22}^k + \rho_{44}^k\right)e^{ik(m-n)} + \rho_{32}^k e^{ik(m+n)} + \rho_{23}^k e^{-ik(m+n)} + \left(\rho_{33}^k + \rho_{44}^k\right)e^{-ik(m-n)}$$

$$= \frac{2}{L}\sum_{k>0}\rho_{44}^k\cos\left(k(m-n)\right) + \frac{1}{L}\sum_{k>0}\left\{\rho_{22}^k e^{ik(m-n)} + \rho_{33}^k e^{-ik(m-n)}\right\} \tag{S25}$$

$$F_{mn}(t) = \frac{2}{L}\sum_{k>0}\rho_{14}^k\sin\left(k(m-n)\right) \tag{S26}$$

where $m,n = 1,2,3,\ldots \ell$ and the time dependence comes from the time dependent matrix elements $\rho_{ij}^k(t)$ of the density matrix $\rho_k(t)$. Note that in arriving at the final form of the Eq. (S25), we have used the fact that $\rho_{23}^k(t) = \rho_{32}^k(t) = 0$ valid for the present choice of initial conditions (see Eq. (S13)). In the unitary case ($\kappa = 0$), $\rho_{22}^k(t)$ and $\rho_{33}^k(t)$ vanish, rendering a simpler form of the $C_{mn}(t)$.

In our numerical scheme, by solving Eqs. (S12), we shall construct the density matrix given in the Eq. (S13) and hence evaluate Eq. (S25) and Eq. (S26). Having the values of TPCs $C_{mn}(t)$ and $F_{mn}(t)$, we construct the correlation (or covariance) matrix $\mathbb{C}_\ell$ (Eq. [12] in the main text) and proceed to calculate the von-Neumann entropy $S(\rho_l)$ of the reduced density matrix ρ_ℓ of a sub-system of size ℓ as

$$S(\rho_\ell) = -\sum_{i=1}^{2\ell}\lambda_i\ln\lambda_i \tag{S27}$$

where λ_i are the eigenvalues of the correlation matrix $\mathbb{C}_\ell$ [S7].
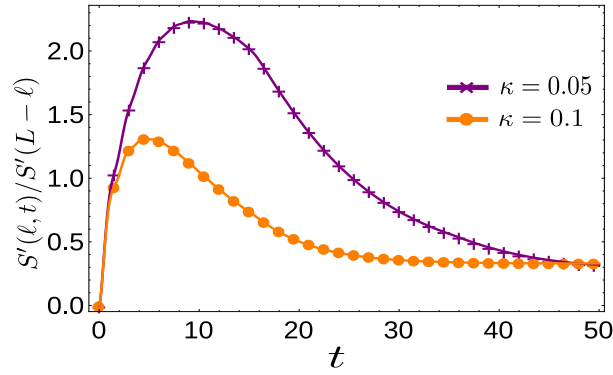
FIG. S1.   (Color online) This figure shows that $S'(\ell, t)$ (denoted by solid lines) is equal to $S'(L - \ell, t)$ (denoted by markers) for all instants of time. We have chosen two values of the coupling strength $\kappa = 0.05$ and 0.1, the sub-system size $\ell = 30$ and the composite system size $L = 100$

NUMERICAL VERIFICATION OF $S'(\ell, t) = S'(L - \ell, t)$ FOR ALL t

Let us recall, the definition of the mutual information (MI)

$$I(\ell : L - \ell) = S(\rho_\ell) + S(\rho_{L-\ell}) - S(\rho_L), \tag{S28}$$

where $S(\rho_\ell)$, $S(\rho_{L-\ell})$ and $S(\rho_L)$ are the von-Neumann entropy of the sub-system, rest of the system and the composite system, respectively. By splitting the quantity $S(\rho_L)$ into two parts, we can rewrite the above equation in following way

$$I(\ell : L - \ell) = S'(\ell) + S'(L - \ell) \tag{S29}$$

where

$$S'(\ell) = S(\rho_\ell) - \frac{\ell}{L} S(\rho_L), \quad \text{and} \quad S'(L - \ell) = S(\rho_{L-\ell}) - \frac{L - \ell}{L} S(\rho_L). \tag{S30}$$

Interestingly, for the bath chosen in the present work, the two quantity $S'(\ell)$ and $S'(L - \ell)$ are exactly equal in all time as shown in the Fig. S1.

STEADY STATE SOLUTION OF $\rho_k(t)$

In the presence of the dissipative environment, following a sudden quench the system reaches a steady state in the asymptotic limit of time $t \to \infty$. In the present scenario, analytical form of the steady state density matrix $\rho_k(\infty)$ for each k mode can be exactly calculated by putting $d\rho_k(t)/dt = 0$ in the Lindblad master equation (S5). The non-zero elements of the density matrix $\rho_k(\infty)$ assume the following form:

$$\rho_{11}(\infty) = \frac{\Delta^2 + 4\epsilon^2 + \kappa^2}{4(\Delta^2 + \epsilon^2) + \kappa^2}, \tag{S31}$$

$$\rho_{22}(\infty) = \rho_{33}(\infty) = \rho_{44}(\infty) = \frac{\Delta^2}{4(\Delta^2 + \epsilon^2) + \kappa^2}, \tag{S32}$$

$$\rho_{14}(\infty) = \frac{\Delta(2\epsilon - i\kappa)}{4(\Delta^2 + \epsilon^2) + \kappa^2}, \tag{S33}$$

where $\epsilon = \mu_f - \cos k$ and $\Delta = \sin k$. These solutions enable us to calculate the steady state two point correlations $C_{mn}(\infty)$, $F_{mn}(\infty)$ and the steady state von Neumann entropy $S(\ell, \infty)$ of a sub-system of size ℓ. Further, the steady state MI $S'(\ell, t)$, calculated using Eq. (S30), is shown in the Fig. S2; this steady state value satisfies an area law in the thermodynamic limit.
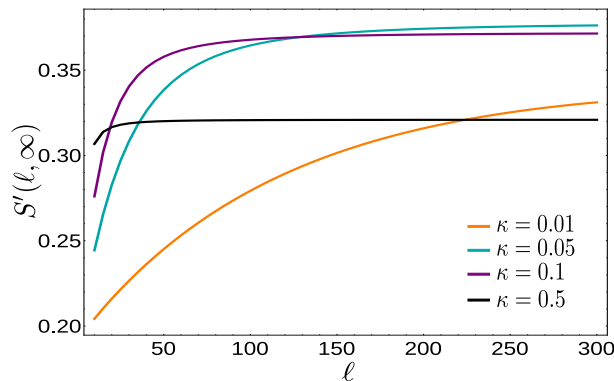
FIG. S2. (Color online) The variation of the steady state value of MI $S'(\ell, t)$ (i.e., $\mathcal{P}(\ell, \kappa)$ in Eq. [12] of the main text) with ℓ for different values of κ. As κ increases from 0 to higher values, $\mathcal{P}(\ell, \kappa)$ apparently shows a sub-volume behavior. In the thermodynamic limit the quantity however satisfies an area law as a consequence of finite ξ_k.. Here, we choose $L = 1000$.
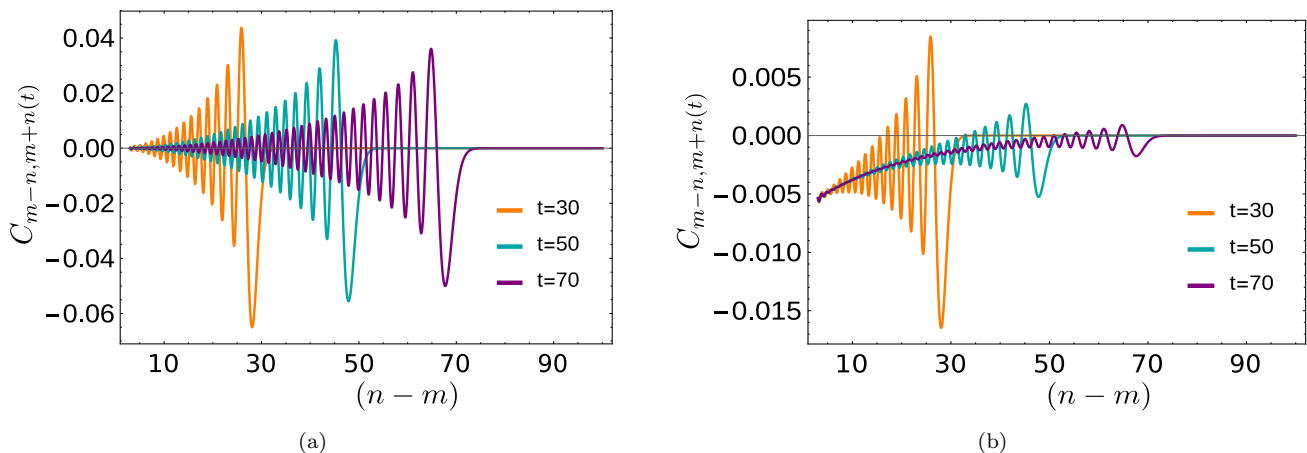

FIG. S3. (Color online). Here, we plot the two-point correlations $C_{mn}(t)$ between pairwise points (labelled by n) equidistant from the site m (chosen to be $m = 50$) for different instants of time after the sudden quench of the chemical potential for (a) the unitary case ($\kappa = 0$) and (b) the dissipative case ($\kappa \neq 0$).

STEADY STATE MI FROM TWO-POINT CORRELATIONS

In this section, we study the dynamics of two-point correlations (TPCs) $C_{mn}(t)$ (given in the Eq. (S25)) further to understand the origin of finite non-zero value of the steady state MI for the dissipative case. Here, we calculate the equal-time single particle TPCs between pairwise points equidistant from a fixed site (denoted by m);

$$C_{m-n,m+n}(t) = \langle c^\dagger_{m-n}(t) c_{m+n}(t) \rangle \tag{S34}$$

by varying n (≥ 1). In Fig. S3, we plot $C_{m-n,m+n}(t)$ as a function of $(n-m)$ for different instants of time. The two points $m + n$ and $m - n$ become correlated only when entangled pair of quasi-particles reach the two points simultaneously. This essentially implies that only the quasi-particles originating at the mid point m can contribute to $C_{m-n,m+n}(t)$ at any time $t > 0$. Note that we have ignored possible contributions from the mid-point of the other segment $(L - 2n)$ due to the circular geometry of the chain; this is a valid approximation as $L \gg 2n$. Thus, it is clear that, at a given time t, only the points lying within distance $m - n = v_g t = t$ can have finite pair-wise correlation with their corresponding counter parts in the segment $m + n$, as is clearly seen in Fig S3. As discussed in the main text, the subsequent peaks after the first peak, i.e. within the region $|n - m| < t$, is due to the presence of the slower moving quasi-particles. In the unitary case (see Fig. 3(a)), the resultant correlation profile evolves in a packet like fashion with its front end propagating with maximum group velocity ($v_{max} = 1$) while the tail end elongates in time due to the velocity differences between quasi-particles. In the dissipative case, however, the correlation profile evolves with a non-vanishing tail even though its front end continue to propagate with velocity v_{max} but with a rapidly diminishing
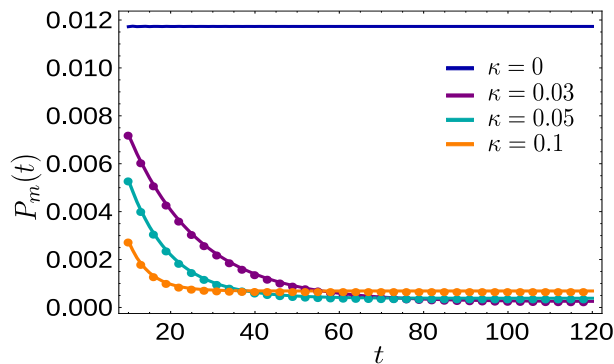
FIG. S4.   (Color online) Here, we plot the quantity $P_m(t)$ with time t for different values of κ. The markers on curves for $\kappa \neq 0$ are obtained using the fitted function $\alpha(\kappa) + \beta(\kappa)\exp(-2\kappa t)$. Here, we have chosen the total system size $L = 1000$.

amplitude (see Fig. S3(b)). It is important to realise that the finite MI observed in the steady state (see Fig. [1] of the main text) is an artefact of this non-vanishing tail of the correlation profile. Further, the surviving TPCs in the steady state is an exponentially decaying function (see Fig. [3] in the main text) with the intermediate distance $|n - m|$ between the two points suggesting the existence of a finite correlation length, $\xi_k = 2/\kappa$, beyond which the TPCs in the steady state have negligible contributions. We have also checked that the real and imaginary part of the other TPC $F_{mn}(t)$ given in Eq. (S26) also has the same dynamical behavior as discussed above.

The scaling of the MI in the steady state with the sub-system size ℓ (see Fig. S2) is now explained as follows. In the steady state, only the points inside the sub-system which are located within a distance ξ_κ from the boundary of the sub-system become correlated with the rest of the system. The two relevant length scales in the steady state are therefore ξ_κ and ℓ. If $\ell \ll \xi_\kappa$, all the points inside the sub-system, contribute to the steady state MI; consequently it *apparently* follows a volume law in this limit. On the other limit, if $\ell \gg \xi_\kappa$, only the points located in the vicinity of the boundary of the sub-system contribute to the steady state MI thus leading to an area law (ℓ independent) behavior in the thermodynamic limit. In the intermediate case when ℓ is comparable with ξ_κ, the steady state MI shows a sub-volume behaviour, as can be seen in Fig. S2.

Finally, we note that the existence of a non-vanishing value of the MI in the steady state despite the quasi-particles having a finite life-time is a striking result in presence of dissipation. We suspect that this happens because the action of the bath is similar to a *continuous* quench on the system which results in generation of quasi-particles at all times. In the steady state, a balance is reached between the generation and destruction processes of the quasi-particles which result in the steady non-vanishing value. Although a rigorous analytical proof of this claim is not feasible, we however, adopt an indirect way to support our claim as follows.

We recall (in the Fig. S3) that as the system evolves, the amplitude of oscillations of TPCs decreases rapidly in the dissipative case unlike the unitary case. To capture this difference in a more compact way, we calculate the following quantity

$$P_m(t) = \sum_{n=m}^{m+v_{max}t} |\langle c_{m-n}^\dagger(t) c_{m+n}(t)\rangle|^2, \qquad v_{max} = 1, \tag{S35}$$

which at a given time can be considered to be a measure of the total number of quasi-particles originated from the point m. In the Fig. S4, we follow the temporal evolution of $P_m(t)$ for different values of κ. In the unitary case ($\kappa = 0$), it remains constant with time which indicates that total number of quasi-particles remains constant for all time; this further implies that the quasi-particles originated by the sudden quench of the chemical potential have infinite life time. However, in the dissipative case ($\kappa \neq 0$), $P_m(t)$ shows an exponential decay to a constant non-zero steady state value. This exponential decay can be interpreted as the result of the decay of the quasi-particles generated due to the sudden quench at $t = 0$. Therefore, for $\kappa \neq 0$, a time scale $\tau_\kappa = 1/2\kappa$ (other than t^*) emerges after which the generation of quasi-particles due to the persistent coupling to the bath and their destruction balances each other, which manifests in the form of a steady value for the MI.
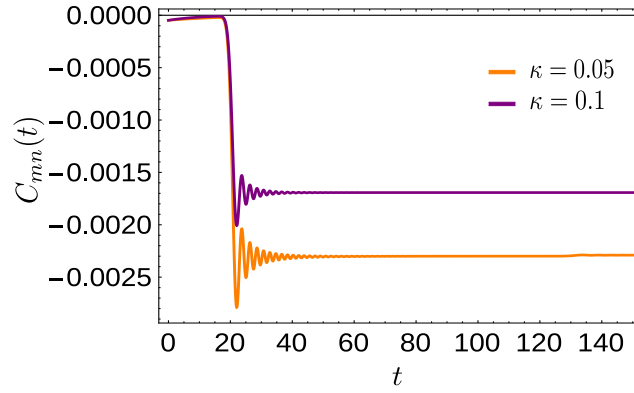
FIG. S5. This figure shows the time evolution of the two point correlation $C_{mn}(t)$ for different values of κ under no quench situation for different values of $(m - n)$. This figure should be compared with Fig. [3] of the main text.

ROLE OF BATH

To comprehend the role played by the bath, we investigate $C_{mn}(t)$ with m and n fixed as a function of time in the *no-quench* situation. In the no-quench situation, there is no quenching of μ and the Kitaev chain is initially prepared in the ground state of Hamiltonian $H_k(\mu)$ with field $\mu = 1$, which thereafter evolves with the same Hamiltonian. After the decay of the (small) initial correlation of the critical ground state, we once again observe that a finite correlation starts developing for $t > t^* = \ell/2$ as depicted in Fig. S5. This, in hindsight, suggests that the action of attaching the bath is similar to a global quench that results in the generation of quasi-particles throughout the system.

[S1] G. Lindblad, Commun. Math. Phys. **48**, 199 (1976).
[S2] C. W. Gardiner and P. Zoller, *Quantum Noise* (Springer, Heidelberg, 2000).
[S3] H. P. Breuer and F. Petruccione, *Theory of open quantum systems*, Oxford University Press, Oxford (2002).
[S4] A. Carmele, M. Heyl, C. Kraus, M. Dalmonte, Phys. Rev. B **92**, 195107 (2015).
[S5] M. Keck, S. Montangero, G. E. Santoro, R. Fazio, D. Rossini, New J. Phys. **19** 113029 (2017).
[S6] S. Bandyopadhyay, S. Laha, U. Bhattacharya and A. Dutta, Sci. Rep. **8**, 11921 (2018).
[S7] I. Peschel, J. Phys. A: Math. Gen. **36**, L205-L208 (2003).